



Selective flotation separation of molybdenite and chalcopyrite using O₃ oxidation method

Hong-tao ZHANG, Xiang-yu SONG, Ye-hao HUANG, Zhen ZHANG, Wen WANG, Lai-fu XU

School of Chemical Engineering, Zhengzhou University, Zhengzhou 450001, China

Received 26 July 2022; accepted 14 February 2023

Abstract: The effect of O₃ oxidation on the flotation recovery of chalcopyrite and molybdenite was investigated. The results of single-mineral flotation tests showed that under the conditions that O₃ concentration was about 90 g/m³ and the gas flow rate was 4 L/min, after chalcopyrite and molybdenite were oxidized for 2 min, the flotation recovery of the chalcopyrite dropped to 16%, while the flotation recovery of molybdenite did not change much. The results of flotation tests for the artificially mixed ores showed that O₃ oxidation pretreatment could replace the Na₂S reagent as a chalcopyrite depressant in the selective flotation separation of chalcopyrite and molybdenite. The contact angle measurements revealed that the O₃ oxidation treatment selectively rendered the surfaces of the chalcopyrite to be hydrophilic. The Zeta potential and X-ray photoelectron spectroscopy analyses revealed that the chalcopyrite surface most likely became hydrophilic due to the formation of water-insoluble hydrophilic oxides and hydroxides on the mineral surface after the oxidation treatment. In addition, although the surface of the molybdenite was slightly oxidized, its surface remained good hydrophobicity.

Key words: chalcopyrite; molybdenite; O₃ oxidation; selective flotation; hydrophilicity

1 Introduction

Molybdenum (Mo) is a very important transition metal element, and molybdenum metal and its alloys are widely used in electronics, metallurgy, chemical industry, national defense, aerospace engineering and other fields [1,2]. Molybdenum minerals are usually associated with copper sulfide minerals [3]. The majority of molybdenum resources are mainly produced from porphyry copper deposits, and it is estimated that about 75% of copper and 50% of molybdenum are derived from such copper ore deposits [4]. The mineral forms of copper and molybdenum in porphyry copper deposits are mainly chalcopyrite and molybdenite, and their similar natural floatabilities make it difficult to separate the two minerals [5–7]. The commonly used method of

separating chalcopyrite and molybdenite is flotation process, that is, to separate one mineral by adding depressants that depress the other mineral. Common chalcopyrite depressants include NaCN, Na₂S, Nokes reagent, and sodium thioglycolate, etc [8–11], and common molybdenite depressants include humic acid, lignosulfonate, dextrin, xanthan gum, pectin, etc [12–16].

At present, the conventional flotation separation of chalcopyrite and molybdenite generally requires the use of large doses of flotation depressants, which will lead to some problems such as high cost, unsafe production process and environmental pollution, etc. So, it is very important to research and develop new separation methods. Pulsating high-gradient magnetic separation (HGMS), flotation in seawater, using nitrogen in flotation, oxidation flotation and thermal pretreatment flotation are all new processes

appearing in recent years [17–19]. Among them, oxidation flotation method has attracted more and more attention because of its low cost, high efficiency and no toxic pollution [20]. The selection of oxidants is crucial for the oxidation flotation methods, such as O_3 , plasma, H_2O_2 , $KMnO_4$, K_2FeO_4 , and electrocatalyst [21–24]. Compared with other oxidants, O_3 has a low price, strong oxidizing ability, and short oxidation time, and the oxidation product is oxygen and will automatically decompose into oxygen in the solution without polluting the environment [25,26]. In the early 1990s, the selective recovery of molybdenite from Cu–Mo bulk concentrates has been studied by the use of O_3 as the depressant of chalcopyrite, but the mechanism was not explained [27]. In addition, related research was carried out but did not achieve a good separation effect. This may be caused by the long contact time between molybdenite and pulp after pretreatment and the low O_3 concentration.

In this study, the possibility of flotation separation for chalcopyrite and molybdenite by using O_3 oxidation was investigated, the feasibility of the method was verified through extensive experiments, the approximate mechanism of the method was analyzed, and whether the method can replace traditional agents was explored by comparing it with the flotation method in which sodium sulfide was used as a chalcopyrite depressant to achieve the effective separation of chalcopyrite and molybdenite.

2 Experimental

2.1 Materials

The pure minerals used in the experiments were chalcopyrite and molybdenite, and both were provided by CMOC Group Limited. Chemical analysis and X-ray diffraction (XRD) patterns confirmed that the purity of the chalcopyrite was above 94% and the purity of the molybdenite was above 93%, which met the testing requirements. Their XRD patterns are presented in Fig. 1. Artificial mixed minerals were made by mixing chalcopyrite with molybdenite in different mass ratios.

The Cu–Mo bulk concentrate used in the experiments assays 1.21 wt.% Cu and 22.03 wt.% Mo, which was produced in a super-large porphyry copper ore processing plant in Luoyang, China.

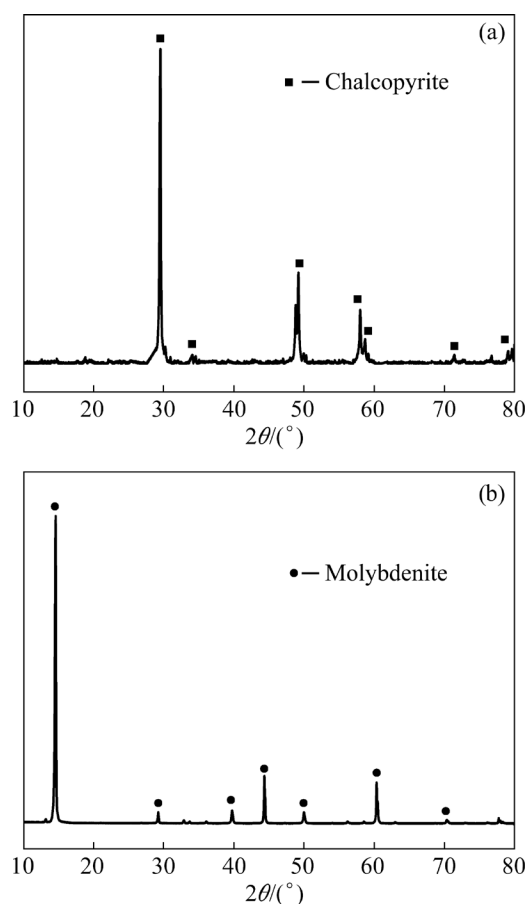


Fig. 1 XRD patterns of prepared ore samples: (a) Chalcopyrite; (b) Molybdenite

2.2 O_3 pretreatment

The O_3 generator used in the experiments was produced by Qingdao Guolin Environmental Protection Technology Co. Ltd. (China). The model number was CF-G-3-20g, the O_3 output was 20 g/h, the O_3 concentration was about 90 g/m^3 , and the gas flow rate was 4 L/min.

First, 3 g of pure minerals were ultrasonically cleaned for 15 min for de-dosing, and then, the minerals were poured into water and the pH was adjusted to 9 by adding sodium hydroxide and hydrochloric acid. The temperature was maintained at about $25 \text{ }^\circ\text{C}$. Finally, O_3 was introduced for the oxidation pretreatment, after which the minerals were transferred to the flotation tube for the flotation stage of the experiment.

2.3 Contact angle measurements

The blocky minerals containing chalcopyrite and molybdenite were cut using a metallographic specimen cutter and then polished with 100, 400, 800, 1200, and 3000 grit sandpaper. The treated

chalcopyrite and molybdenite ore blocks were cleaned using an ultrasonic cleaner for 5 min. Then, they were pretreated via O₃ oxidation for different durations of time. Finally, the contact angles of the chalcopyrite and molybdenite ore subjected to oxidation pretreatment for different durations of time were measured using a contact angle measuring instrument.

2.4 Zeta potential measurements

The pure chalcopyrite and molybdenite with and without oxidation were weighed, 0.04 g of each were placed in four 50 mL beakers, 40 mL of 0.001 mol/L KNO₃ solution were added to the beakers, and the mixture was sonicated for 2 min. Then, the solutions were adjusted to different pH values (5, 7, 9, 10, and 11) using NaOH and HCl, were sonicated for 13 min and left to stand for 5 min, and 10 mL of supernatant was collected. The supernatant was removed from the sample and allowed to stand in a centrifuge tube for 24 h. The zeta potentials of the minerals were measured using a Nano ZS90 potential and particle size analyzer (Malvern, UK), and the average of six measurements was taken as the value.

2.5 X-ray photoelectron spectroscopy

The pure minerals were ground using an agate mill until more than 90% of the specimen was <0.074 mm in size. The milled minerals were cleaned via ultrasonication for 2 min in a beaker containing 50 mL of 1 mol/L HNO₃, after which a portion of the minerals was removed and the chalcopyrite and molybdenite were analyzed via X-ray photoelectron spectroscopy (XPS) without oxidation. Another portion of the cleaned minerals was poured into water and then pH was adjusted to 9 with sodium hydroxide and hydrochloric acid, followed by an O₃ oxidation pretreatment. After 2 min of oxidation pretreatment, the minerals were removed and the chalcopyrite and molybdenite were analyzed via XPS. The collected data were analyzed using the Avantage software and were calibrated with C 1s (284.8 eV) in combination with energy.

2.6 Flotation study

The pure mineral and artificially mixed ore flotation experiments were performed using Hallimond flotation tubes. In each experiment,

3.00 g of minerals were weighed and sonicated for 15 min, after which the minerals were transferred to the flotation tubes, and about 100 mL of water was added. Then, the pH was adjusted with NaOH and HCl, the solution was stirred for 5 min, and kerosene and terpenic oil were added in turn for 3 min each. Finally, the froth product and tailings were obtained by flotation for 3 min. The artificially mixed mineral flotation test was prepared by mixing chalcopyrite and molybdenite with different mass ratios to create the mineral samples, and the rest of the procedure was the same as the above-described method.

The flotation experiments of Cu–Mo bulk concentrates were performed using RK/FD-II type 0.5 L flotation machine. In each experiment, 78 g of minerals were weighed after which the minerals were transferred to the flotation machine and about 500 mL of water was added. Then, the pH was adjusted with NaOH and HCl, the solution was stirred for 5 min, and kerosene and terpenic oil were added in turn for 3 min each. Finally, the froth product and tailings were obtained by flotation for 3 min.

Both Cu and Mo grade and S concentration were measured using ICP.

3 Results and discussion

3.1 Pure mineral flotation test

A controlled variable method was used to explore suitable testing conditions. The effect of the kerosene dosage on the flotation recovery of chalcopyrite and molybdenite, without O₃ oxidation, and with a terpenic oil dosage of 20 mg/L and pH 7 is shown in Fig. 2. The effect of pH on the floatability of chalcopyrite and molybdenite without O₃ oxidation, with a kerosene dosage of 60 mg/L and a terpenic oil dosage of 20 mg/L is shown in Fig. 3. The effect of the O₃ oxidation pretreatment time on the floatability of chalcopyrite and molybdenite with a pH of 9, a kerosene dosage of 60 mg/L and a terpenic oil dosage of 20 mg/L is shown in Fig. 4.

As shown in Fig. 2, as the kerosene dosage increased, the recovery of chalcopyrite and molybdenite via flotation increased. The recovery of molybdenite increased significantly when the kerosene dosage was less than 60 mg/L and only increased slightly after the kerosene dosage reached

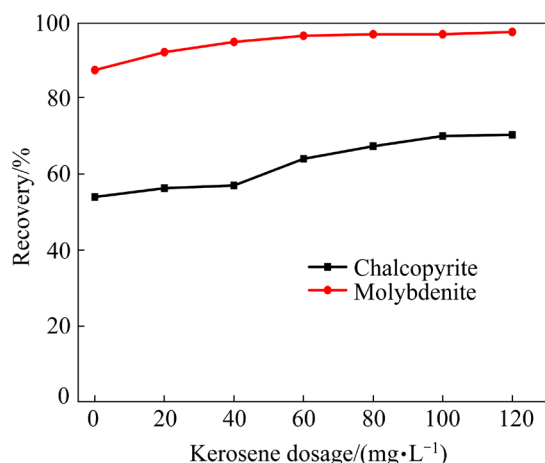


Fig. 2 Effect of kerosene dosage on flotation recovery of chalcopyrite and molybdenite

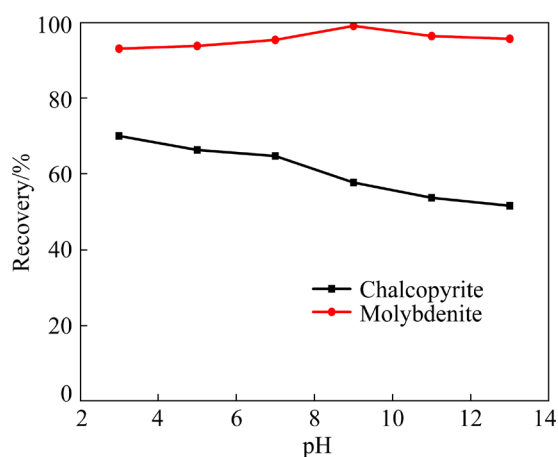


Fig. 3 Flotation recovery of molybdenite and chalcopyrite as function of pH

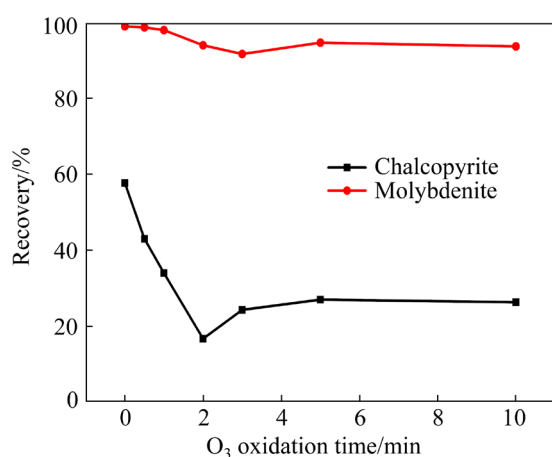


Fig. 4 Effect of O₃ oxidation time on flotation recovery of chalcopyrite and molybdenite

60 mg/L. As shown in Fig. 3, as the pH increased, the recovery of chalcopyrite decreased, and the recovery of molybdenite initially increased and then

decreased. As Fig. 4 shows, the recovery of chalcopyrite decreased significantly with increasing O₃ oxidation pretreatment time. The recovery reached a minimum of 16% for an oxidation time of 2 min. The flotation recovery of chalcopyrite increased slightly afterward, which may be due to the desorption of oxidation products on the surface of chalcopyrite. The recovery of molybdenite only changed slightly after the oxidation pretreatment, and it still exceeded 90%.

3.2 Flotation separation of artificially mixed ore

The results of the flotation separation tests for different proportions of artificially mixed ore with a pH of 9, oxidation time of 2 min, sodium sulfide dosage of 100 mg/L, kerosene dosage of 60 mg/L, and terpenic oil dosage of 20 mg/L are presented in Table 1. The chalcopyrite to molybdenite ratio was 1:1 for artificially mixed Ore 1, 3:1 for artificially mixed Ore 2, and 5:1 for artificially mixed Ore 3.

Table 1 shows that as the proportion of chalcopyrite in the artificially mixed ore increased, the molybdenum grade of the flotation concentrate product gradually decreased and the copper grade gradually increased for both the sodium sulfide and O₃ oxidation treatment flotation experiments. Moreover, the molybdenum recovery did not change much and remained at about 90%. The copper grade of the tailings (copper concentrate) increased and the molybdenum grade of the tailings decreased, and the copper recovery was greater than 90% for both. Both flotation separation methods achieve the effective separation of chalcopyrite and molybdenite to different degrees, which is consistent with the results of the single mineral flotation experiments.

The above experimental results demonstrate that the depression effect of the O₃ oxidation on the chalcopyrite is similar to that of sodium sulfide. They can both achieve effective separation of chalcopyrite and molybdenite, but sodium sulfide has the disadvantage of high dosage, large cost, and environmental pollution. So, O₃ can replace Na₂S reagent as a copper depressant in selective flotation of chalcopyrite and molybdenite.

3.3 Flotation separation of Cu–Mo bulk concentrates

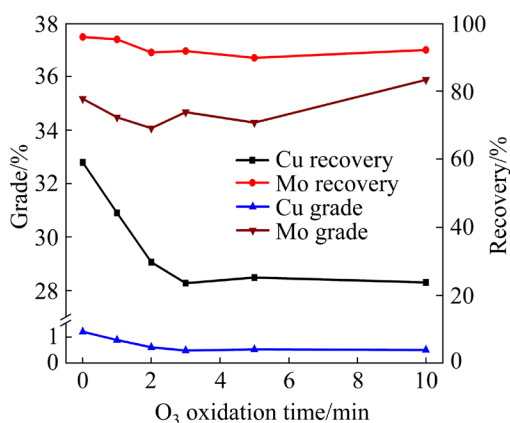
The effect of the O₃ oxidation pretreatment time on the flotation separation result of Cu–Mo

Table 1 Flotation separation results of artificially mixed ores in different proportions by O₃ oxidation and sodium sulfide

Ore	Processing condition	Product	Yield/%	Grade/%		Recovery/%	
				Cu	Mo	Cu	Mo
1	O ₃ oxidation	Concentrate	48.00	3.15	52.76	9.27	90.28
		Tailings	52.00	28.46	5.24	90.73	9.72
		Feed	100.00	16.31	28.05	100.00	100.00
	Sodium sulfide	Concentrate	46.33	1.49	55.12	4.23	91.05
		Tailings	53.67	29.11	4.68	95.77	8.95
		Feed	100.00	16.31	28.05	100.00	100.00
2	O ₃ oxidation	Concentrate	25.00	6.77	51.15	6.92	91.21
		Tailings	75.00	30.36	1.53	93.08	8.19
		Feed	100.00	24.46	14.02	100.00	100.00
	Sodium sulfide	Concentrate	23.67	4.67	52.91	4.52	89.32
		Tailings	76.33	30.60	1.96	95.48	10.68
		Feed	100.00	24.46	14.02	100.00	100.00
3	O ₃ oxidation	Concentrate	17.67	8.10	48.54	5.26	91.72
		Tailings	81.33	31.28	0.94	94.74	8.28
		Feed	100.00	27.18	9.35	100.00	100.00
	Sodium sulfide	Concentrate	16.33	6.18	50.43	3.71	88.10
		Tailings	81.67	31.41	1.33	96.29	11.90
		Feed	100.00	27.18	9.35	100.00	100.00

bulk concentrates with a pH of 9, a kerosene dosage of 60 mg/L, and a terpenic oil dosage of 20 mg/L is shown in Fig. 5.

As Fig. 5 shows, with the increase of O₃ oxidation time, the recovery and grade of copper in concentrate firstly decreased significantly, and then basically tended to be stable, with the lowest being 23.61% and 16%, respectively, when the oxidation time was 3 min, and then kept basically unchanged.

**Fig. 5** Effect of O₃ oxidation time on flotation separation results of Cu–Mo bulk concentrates

The recovery and grade of molybdenum in the concentrate after oxidation pretreatment only changed slightly. When the O₃ oxidation time was 3 min, recovery rate and grade of molybdenum in the concentrate were 91.77% and 34.67%, respectively. This is consistent with the above results.

3.4 Mechanism of chalcopyrite and molybdenite separation via O₃ oxidation

3.4.1 Contact angle

The floatability of a mineral is influenced by the surface wettability, which can be estimated from the surface contact angle. The variations in the contact angles of chalcopyrite and molybdenite after different O₃ oxidation treatment time are presented in Fig. 6.

It can be seen from Fig. 6 that the contact angles of the untreated chalcopyrite and molybdenite were 74° and 70°, respectively. The contact angle of chalcopyrite decreased significantly with increasing O₃ oxidation time, and it finally stabilized at about 30°. The contact angle

of molybdenite did not change significantly and remained at about 70° , which may be due to the hydrophilic oxidation products on the surfaces of the molybdenite dissolved in the water. This means that the chalcopyrite surfaces became more hydrophilic after the O_3 oxidation pretreatment, while the molybdenite surfaces did not change significantly, which is consistent with the results of the previous flotation tests.

3.4.2 Zeta potential

Figure 7 shows the variations in the Zeta potential with the pH of the surfaces of the chalcopyrite and molybdenite with and without O_3 oxidation pretreatment.

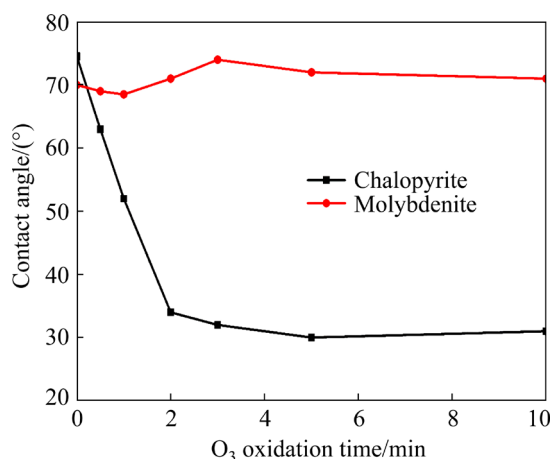


Fig. 6 Contact angles of chalcopyrite and molybdenite after different O_3 oxidation pretreatment time

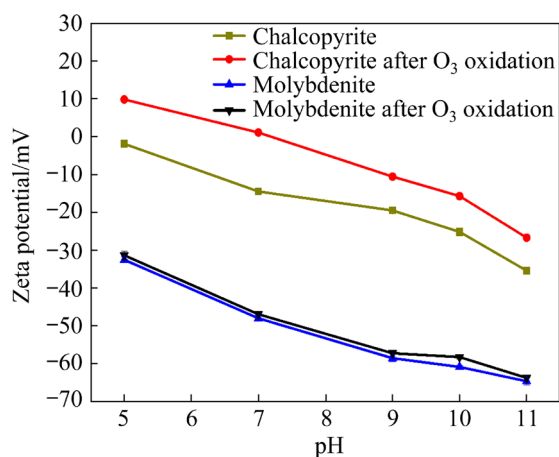


Fig. 7 Zeta potentials of molybdenite and chalcopyrite with and without O_3 oxidation pretreatment as function of pH

As can be seen from Fig. 7, Zeta potentials of all samples decreased with increasing pH, and Zeta potential of chalcopyrite was higher than that of molybdenite with and without O_3 oxidation

pretreatment. In the case of chalcopyrite, Zeta potential of the surfaces of the chalcopyrite increased substantially after the O_3 oxidation pretreatment. This may be due to the adsorption of the oxidation products onto the surfaces of the chalcopyrite, which increased the electronegativity of the surface of the chalcopyrite. In the case of molybdenite, Zeta potential of the surfaces of the molybdenite after the O_3 oxidation pretreatment only increased slightly. Overall, the increase in the zeta potential of the chalcopyrite surfaces after the O_3 oxidation pretreatment was significantly higher than that of the molybdenite surfaces, which is consistent with the results of the previous flotation tests.

3.4.3 XPS results

To investigate the effect mechanism of O_3 pretreatment on the floatability of chalcopyrite and molybdenite, the chalcopyrite and molybdenite with and without O_3 oxidation pretreatment were analyzed via XPS, and the results are presented in Figs. 8 and 9. Figure 8 presents the XPS spectra of Cu 2p, Fe 2p, S 2p, and O 1s for chalcopyrite without pretreatment and with 2 min of O_3 oxidation. Figure 9 presents the spectra of Mo 3d, S 2p, and O 1s for the molybdenite without pretreatment and after 2 min of O_3 oxidation.

Figure 8(a) presents the Cu 2p high-resolution spectrum of chalcopyrite with and without O_3 oxidation pretreatment. As shown, the binding energy peak at 932.2 eV for the untreated chalcopyrite corresponds to Cu(I) [28], indicating that the copper in the chalcopyrite is present as Cu(I). The peak intensity of Cu(I) decreases and the Cu(II) peak appears in the chalcopyrite spectrum after O_3 oxidation pretreatment, indicating the oxidation of copper on the surface of the chalcopyrite, and the binding energy peaks of Cu(II) match those of CuO [29] and $Cu(OH)_2$ [30]. Figure 8(b) shows the Fe 2p high-resolution spectra of chalcopyrite with and without O_3 oxidation pretreatment. The peak of untreated chalcopyrite at 708.1 eV corresponds to $CuFeS_2$ [24]. The intensity of this peak is significantly reduced after the oxidative pretreatment, and new peaks appear at 711.8 and 713.7 eV, corresponding to FeOOH [31] and iron sulfate $Fe_2(SO_4)_3$ [24], respectively. Figure 8(c) presents the high-resolution spectra of the S 2p in the chalcopyrite with and without O_3 oxidation pretreatment. The S on the surface of the

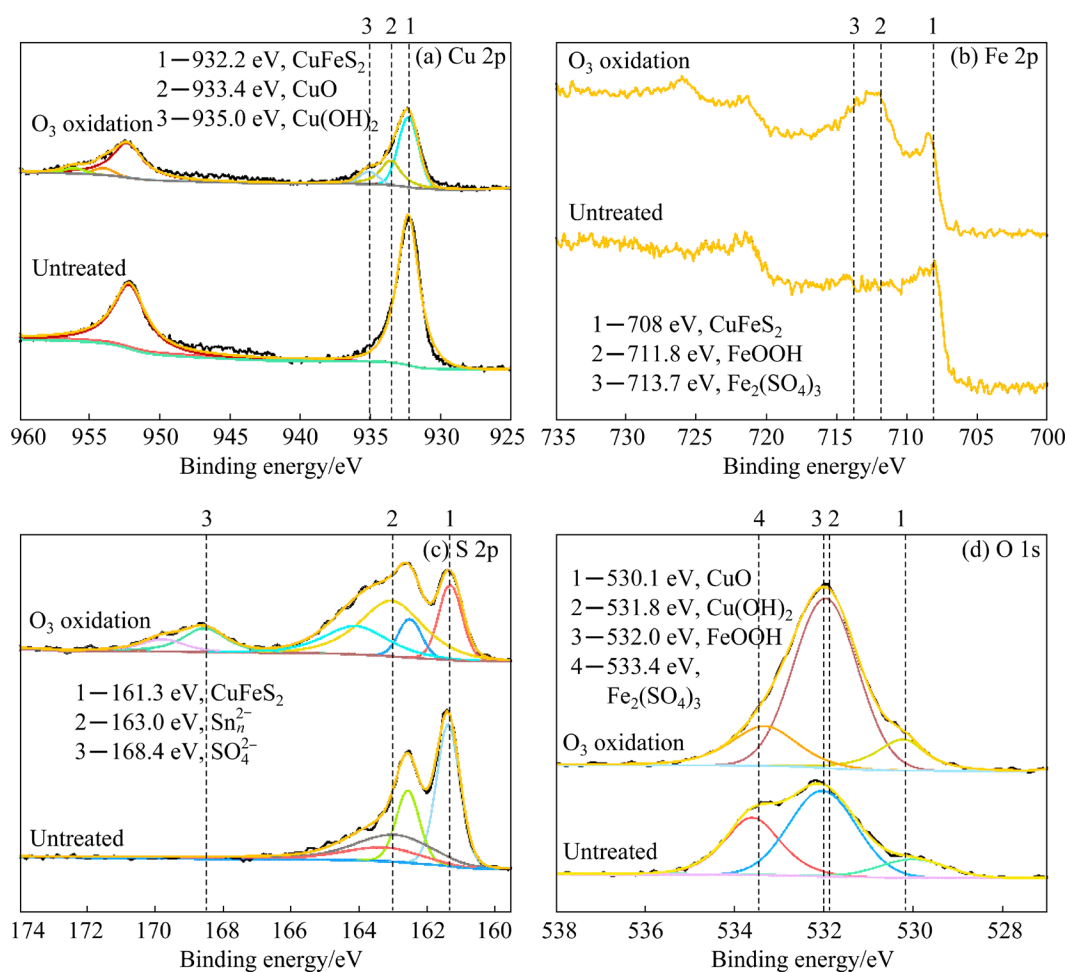


Fig. 8 XPS spectra of chalcopyrite with and without O₃ oxidation: (a) Cu 2p; (b) Fe 2p; (c) S 2p; (d) O 1s

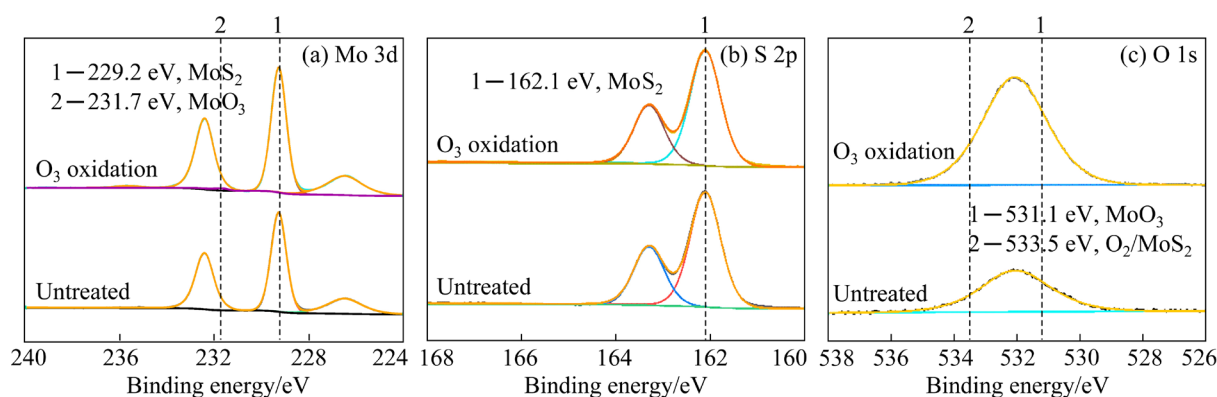


Fig. 9 XPS spectra of molybdenite with and without O₃ oxidation: (a) Mo 3d; (b) S 2p; (c) O 1s

untreated chalcopyrite is mainly CuFeS₂ [32] and S_n²⁻ [33]. The intensities of these two peaks decrease after the oxidation treatment, and a new peak appears at 168.4 eV, corresponding to sulfate SO₄²⁻ [34]. Figure 8(d) presents the O 1s high-resolution spectra of chalcopyrite with and without O₃ oxidation pretreatment. As can be seen, new peaks appear after the O₃ oxidation pretreatment,

corresponding to CuO [35], Cu(OH)₂ [36], FeOOH [37], and SO₄²⁻ [28].

Figure 9(a) shows the Mo 3d high-resolution spectrum of molybdenite with and without O₃ oxidation pretreatment. The untreated molybdenite has a peak centered at a binding energy of 229.2 eV, corresponding to molybdenite (MoS₂) [38]. The oxidation pretreatment does not change the

intensity of this peak significantly, but a very small new peak appears at a binding energy of 231.7 eV, corresponding to MoO_3 [38]. It can be seen from the S 2p high-resolution spectra of molybdenite with and without O_3 oxidation pretreatment (Fig. 9(b)), that the S on the surface of the molybdenite with and without oxidation pretreatment remains essentially unchanged, and both of the peaks at 162.1 eV correspond to molybdenite (MoS_2) [39]. Figure 9(c) presents the O 1s high-resolution spectra of molybdenite with and without O_3 oxidation. The oxidation pretreatment increases the intensity of the peaks significantly, indicating that the molybdenite surfaces are oxidized. The binding energy peak at 531.2 eV corresponds to MoO_3 , and the binding energy peak at 533.5 eV corresponds to the oxygen attached to the molybdenite surfaces [40].

In summary, both chalcopyrite and molybdenite were oxidized during the O_3 oxidation pretreatment, and the degree of oxidation on the chalcopyrite surfaces was greater than that of the molybdenite surfaces. The oxidation of the chalcopyrite produced hydrophilic oxidation products, i.e., CuO , $\text{Cu}(\text{OH})_2$, FeOOH , and $\text{Fe}_2(\text{SO}_4)_3$, which were adsorbed onto the surfaces of the chalcopyrite and decreased its floatability. The oxidation product (MoO_3) on the surface of molybdenite was less abundant, so it caused only partial oxidation of the molybdenite and the dissolution of MoO_3 in the water. In addition, the S on the surfaces of the molybdenite remained basically unchanged, which might be another reason that the floatability of the molybdenite don't change significantly.

Figure 10 indicates the $\text{pH}-\phi_h$ diagrams for copper, iron, and molybdenum. Under general oxidation and flotation conditions, the dominant dissolved ion species are molybdenum, and the dominant solid species are copper and iron, as they remain solids or precipitates [21]. This can be explained as follows. The oxidation products on the surface of molybdenite dissolve in solution, while some of the copper and iron products on the surface of chalcopyrite do not dissolve and immediately precipitate as copper oxide and/or iron hydroxide, which may affect the surface characteristics.

By combining XPS results and $\text{pH}-\phi_h$ diagrams, it can be concluded that O_3 can react with

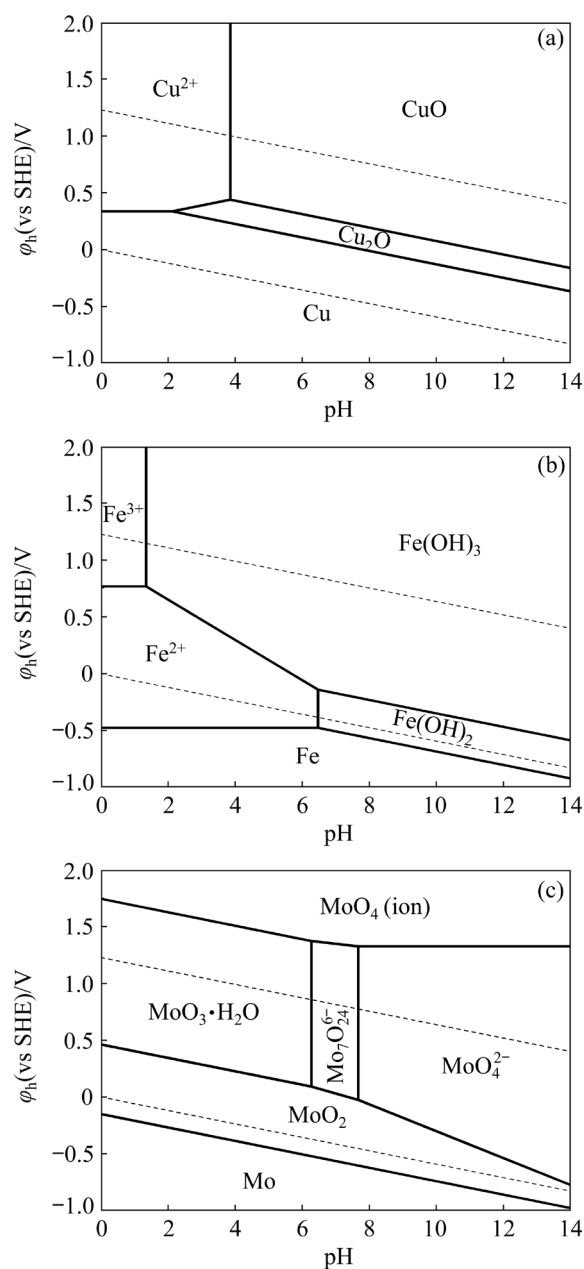
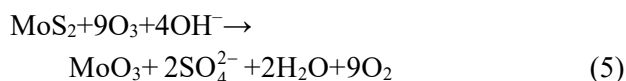
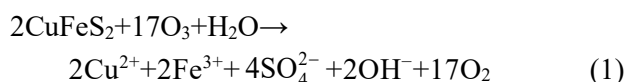
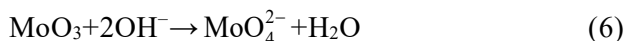


Fig. 10 Calculation result of equilibrium of chemical species as $\text{pH}-\phi_h$ diagrams: (a) Copper; (b) Iron; (c) Molybdenum

chalcopyrite and molybdenite in solution, and the reactions in solution may be [41]





Next, 0.01 mol chalcopyrite and molybdenite in 1 L solution with pH 9 were pretreated via O_3 oxidation (adjusted using NaOH and HCl). The variations in the sulfur concentrations of the solution with time are presented in Fig. 11.

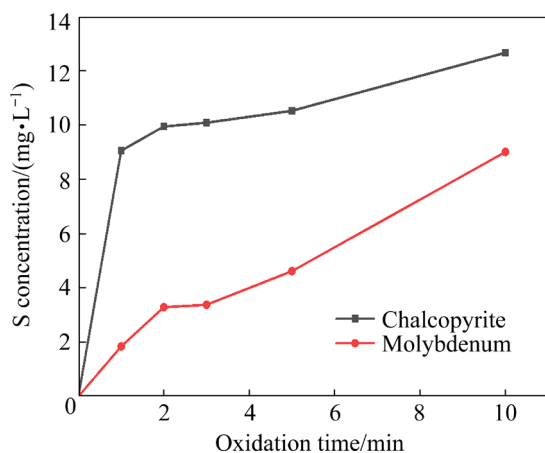


Fig. 11 S concentration in solutions of chalcopyrite and molybdenite at different oxidation time

It can be seen from Fig. 11 that the oxidation of chalcopyrite is significantly larger than that of molybdenite at a reaction time of 2 min. This is consistent with the above results.

4 Conclusions

(1) O_3 has the advantages of low price, strong oxidation ability, and short oxidation time. O_3 oxidation can selectively depress the floatability of chalcopyrite, while it has little effect on the floatability of molybdenite.

(2) The single-mineral flotation tests revealed that the O_3 oxidation pretreatment significantly reduced the flotation recovery of chalcopyrite even in the presence of a trap but had little effect on that of molybdenite. The artificially mixed ore flotation tests revealed that the O_3 oxidation could achieve selective flotation separation of chalcopyrite and molybdenite, and its effect was as good as that of sodium sulfide. The flotation results of Cu–Mo bulk concentrates showed that O_3 oxidation could selectively separate chalcopyrite and molybdenite.

(3) The contact angle and Zeta potential results showed that the O_3 oxidation treatment selectively made the chalcopyrite surface hydrophilic, while molybdenite remained hydrophobic. The X-ray

photoelectron spectroscopy results indicated that the reason for this selective flotation separation may be that the hydrophilic oxidation products (CuO , $\text{Cu}(\text{OH})_2$, FeOOH , and $\text{Fe}_2(\text{SO}_4)_3$) of the chalcopyrite oxidation adsorb onto the surfaces of the chalcopyrite, reducing the floatability of the chalcopyrite; while the oxidation product (MoO_3) of molybdenite dissolves in water and has little effect on the floatability of the molybdenite.

(4) The results indicate that the O_3 oxidation pretreatment flotation separation of chalcopyrite and molybdenite is promising chalcopyrite and molybdenite separation method.

CRedit authorship contribution statement

Hong-tao ZHANG: Visualization, Methodology, Data curation, Writing – Original draft; **Xiang-yu SONG:** Conceptualization, Visualization, Investigation; **Ye-hao HUANG:** Visualization, Investigation, Software; **Zhen ZHANG:** Investigation, Software; **Wen WANG:** Investigation, Software; **Lai-fu XU:** Software.

Declaration of competing interest

The authors declare no competing financial interests or personal relationships that could have appeared to influence the work reported in this paper.

Acknowledgments

The authors gratefully acknowledge the financial support from the National Natural Science Foundation of China (No. 51874259).

References

- [1] PARK I, HONG S, JEON S, ITO M, HIROYOSHI N. A review of recent advances in depression techniques for flotation separation of Cu–Mo sulfides in porphyry copper deposits [J]. *Metals*, 2020, 10: 1269–1295.
- [2] CAO Fei, WANG Wei, WEI De-zhou, LIU Wen-gang. Separation of tungsten and molybdenum with solvent extraction using functionalized ionic liquid tricaprilmethylammonium bis(2,4,4-trimethylpentyl) phosphinate [J]. *International Journal of Minerals Metallurgy and Materials*, 2021, 28: 1769–1776.
- [3] CASTRO S, LOPEZ-VALDIVIESO A, LASKOWSKI J S. Review of the flotation of molybdenite. Part I: Surface properties and floatability [J]. *International Journal of Mineral Processing*, 2016, 148: 48–58.
- [4] YANG Bing-qiao, YAN Hai, ZENG Meng-yuan, ZHU Huan-yu. Tiopronin as a novel copper depressant for the selective flotation separation of chalcopyrite and molybdenite [J]. *Separation and Purification Technology*, 2021, 266: 118576.

- [5] MIKI H, HIRAJIMA T, MUTA Y, SUYANTARA G P W, SASAKI K. Effect of sodium sulfite on floatability of chalcopyrite and molybdenite [J]. *Minerals*, 2018, 8: 172–183.
- [6] BAHRAMI A, MIRMOHAMMADI M, GHORBANI Y, KAZEMI F, ABDOLLAHI M, DANESH A. Process mineralogy as a key factor affecting the flotation kinetics of copper sulfide minerals [J]. *International Journal of Minerals Metallurgy and Materials*, 2019, 26: 430–439.
- [7] CAO Fei, SUN De-si, QIU Xian-hui, ZHOU De-zhi, ZHANG Xing-rong, SUN Chuan-yao. Synthesis of novel thionocarbamate for copper–sulfur flotation separation and its adsorption mechanism [J]. *Transactions of Nonferrous Metals Society of China*, 2020, 32: 2709–2718.
- [8] PRASAD M S. Reagents in the mineral industry-recent trends and applications [J]. *Minerals Engineering*, 1992, 5: 279–294.
- [9] QIN Wen-qing, WU Jia-jia, JIAO Fen, ZENG Jin-ming. Mechanism study on flotation separation of molybdenite from chalcocite using thioglycollic acid as depressant [J]. *International Journal of Mining Science and Technology*, 2017, 27: 1043–1049.
- [10] GUO Bao, PENG Yong-jun, ESPINOSA-GOMEZ R. Cyanide chemistry and its effect on mineral flotation [J]. *Minerals Engineering*, 2014, 66/67/68: 25–32.
- [11] TAHERI B, ABDOLLAHY M, TONKABONI S Z S, JAVADIAN S, YARAHMADI M. Dual effects of sodium sulfide on the flotation behavior of chalcopyrite. I: Effect of pulp potential [J]. *International Journal of Minerals Metallurgy and Materials*, 2014, 21: 415–422.
- [12] YANG Bing-qiao, ZENG Meng-yun, ZHU Huan-yu, HUANG Peng-liang, LI Zhi-li, SONG Shao-xian. Selective depression of molybdenite using a novel eco-friendly depressant in Cu–Mo sulfides flotation system [J]. *Colloids and Surfaces A: Physicochemical and Engineering Aspects*, 2021, 622: 126683.
- [13] YAN Hai, YANG Bing-qiao, ZENG Meng-yuan, HUANG Peng-liang, TENG Ai-ping. Selective flotation of Cu–Mo sulfides using xanthan gum as a novel depressant [J]. *Minerals Engineering*, 2020, 156: 106486.
- [14] YUAN Duo-wei, KADIEN K, LIU Qi, ZENG Hong-bao. Selective separation of copper–molybdenum sulfides using humic acids [J]. *Minerals Engineering*, 2019, 133: 43–46.
- [15] BEAUSSART A, PARKINSON L, MIERCZYNSKA-VASILEV A, BEATTIE D A. Adsorption of modified dextrans on molybdenite: AFM imaging, contact angle, and flotation studies [J]. *Journal of Colloid and Interface Science*, 2012, 368: 608–615.
- [16] ANSARI A, PAWLIK M. Floatability of chalcopyrite and molybdenite in the presence of lignosulfonates. Part II: Hallimond tube flotation [J]. *Minerals Engineering*, 2006, 20: 609–616.
- [17] CHEN Lu-zheng, XIONG Tao, XIONG Da-he, YANG Ruo-yu, PENG Yuan-lun, SHAO Yan-hai, XU Jin-yue, ZENG Jian-wu. Pulsating hgms for industrial separation of chalcopyrite from fine copper–molybdenum co-flotation concentrate [J]. *Minerals Engineering*, 2021, 170: 106967.
- [18] TANG Xue-kun, CHEN Yan-fei, LIU Kun, ZENG Guang-sheng, PENG Qian, LI Zi-shun. Selective flotation separation of molybdenite and chalcopyrite by thermal pretreatment under air atmosphere [J]. *Colloids and Surfaces A: Physicochemical and Engineering Aspects*, 2019, 583: 123958.
- [19] MIKI H, MATSUOKA H, HIRAJIMA T, SUYANTARA G P W, SASAKI K. Electrolysis oxidation of chalcopyrite and molybdenite for selective flotation [J]. *Materials Transactions*, 2017, 58: 761–767.
- [20] SUYANTARA G P W, HIRAJIMA T, MIKI H, SASAKI K, YAMANE M, TAKIDA E, KUROIWA S, IMAIZUMI Y. Selective flotation of chalcopyrite and molybdenite using H₂O₂ oxidation method with the addition of ferrous sulfate [J]. *Minerals Engineering*, 2018, 122: 312–326.
- [21] HIRAJIMA T, MORI M, ICHIKAWA O, SASAKI K, MIKI H, FARAHAT M, SAWADA M. Selective flotation of chalcopyrite and molybdenite with plasma pre-treatment [J]. *Minerals Engineering*, 2014, 66/67/68: 102–111.
- [22] LIAO Run-peng, FENG Qi-cheng, WEN Shu-ming, LIU Jian. Flotation separation of molybdenite from chalcopyrite using ferrate(VI) as selective depressant in the absence of a collector [J]. *Minerals Engineering*, 2020, 152: 106369.
- [23] PENG Wei-jun, LIU Shu-guang, CAO Yi-jun, WANG Wei, LU Shuai, HUANG Yu-kun. A novel approach for selective flotation separation of chalcopyrite and molybdenite–Electrocatalytic oxidation pretreatment and its mechanism [J]. *Applied Surface Science*, 2022, 597: 153753.
- [24] HIRAJIMA T, MIKI H, SUYANTARA G P W, MATSUOKA H, ELMAHDY A M, SASAKI K, IMAIZUMI Y, KUROIWA S. Selective flotation of chalcopyrite and molybdenite with H₂O₂ oxidation [J]. *Minerals Engineering*, 2017, 100: 83–92.
- [25] CRUTCHIK D, FRANCHI O, JEISON D, VIDAL G, PINTO A, PEDROUSO A, CAMPOS J L. Techno-economic evaluation of ozone application to reduce sludge production in small urban WWTPs [J]. *Sustainability*, 2022, 14: 2480–2492.
- [26] SANO N, YAMADA K, SUNTORNLÖHANAKUL T, TAMON H. Low temperature oxidation of Fe-included single-walled carbon nanohorns in water by ozone injection to enhance porous and magnetic properties [J]. *Chemical Engineering Journal*, 2016, 283: 978–981.
- [27] YE Y, JANG W H, YALAMANÇILI M R, MILLER J D. Molybdenite flotation from copper/molybdenum concentrates by ozone conditioning [J]. *Mining, Metallurgy & Exploration*, 1990, 7: 173–179.
- [28] GHAREMANINEZHAD A, DIXON D G, ASSELIN E. Electrochemical and XPS analysis of chalcopyrite (CuFeS₂) dissolution in sulfuric acid solution [J]. *Electrochimica Acta*, 2013, 87: 97–112.
- [29] CAPECE F M, CASTRO V D, FURLANI C, MATTOGNO G, FRAGALE C, GARGANO M, ROSSI M. “Copper chromite” catalysts: XPS structure elucidation and correlation with catalytic activity [J]. *Journal of Electron Spectroscopy and Related Phenomena*, 1982, 27: 119–128.
- [30] BIESINGER M C, LAU L W M, GERSON A R, SMART R S C. Resolving surface chemical states in XPS analysis of first row transition metals, oxides and hydroxides: Sc, Ti, V, Cu and Zn [J]. *Applied Surface Science*, 2010, 257: 887–898.
- [31] BUCKLEY A N, WOODS R. An X-ray photoelectron

- spectroscopic study of the oxidation of chalcopyrite [J]. Australian Journal of Chemistry, 1984, 17: 401–414.
- [32] NAKAI I, SUGITANI Y, NAGASHIMA K, NIWA Y. X-ray photoelectron spectroscopic study of copper minerals [J]. Journal of Inorganic and Nuclear Chemistry, 1978, 40: 789–791.
- [33] HARMER S L, THOMAS J E, FORNASIERO D, GERSON A R. The evolution of surface layers formed during chalcopyrite leaching [J]. Geochimica et Cosmochimica Acta, 2006, 70: 4392–4402.
- [34] SIRIWARDANE R V, COOK J M. Interactions of NO and SO₂ with iron deposited on silica [J]. Journal of Colloid and Interface Science, 1985, 104: 250–257.
- [35] MCINTYRE N S, ZETARUK D G. X-ray photoelectron spectroscopic studies of iron oxides [J]. Analytical Chemistry, 1977, 49: 1521–1529.
- [36] FAZAL M, HASEEB A, MASJUKI H. Corrosion mechanism of copper in palm biodiesel [J]. Corrosion Science, 2013, 67: 50–59.
- [37] TAN B J, KLABUNDE K J, SHERWOOD P M A. X-ray photoelectron spectroscopy studies of solvated metal atom dispersed catalysts. Monometallic iron and bimetallic iron-cobalt particles on alumina [J]. Chemistry of Materials, 1990, 2: 186–191.
- [38] BAKER M A, GILMORE R, LENARDI C, GISSLER W. XPS investigation of preferential sputtering of s from MOS₂ and determination of MOS_x stoichiometry from Mo and S peak positions [J]. Applied Surface Science, 1999, 150: 255–262.
- [39] IRANMAHBOOB J, GARDNER S D, TOGHIANI H, HILL D O. XPS study of molybdenum sulfide catalyst exposed to CO and H₂ [J]. Journal of Colloid and Interface Science, 2004, 270: 123–126.
- [40] SHUXIAN Z, HALL W K, ERTL G, KNÖZINGER H. X-ray photoemission study of oxygen and nitric oxide adsorption on MOS₂ [J]. Journal of Catalysis, 1986, 100: 167–175.
- [41] FAIRTHORNE G, FORNASIERO D, RALSTON J. Effect of oxidation on the collectorless flotation of chalcopyrite [J]. International Journal of Mineral Processing, 1997, 49: 31–48.

O₃ 氧化法选择性浮选分离辉钼矿和黄铜矿

张红涛, 宋翔宇, 黄业豪, 张振, 王文, 徐来福

郑州大学 化学学院, 郑州 450001

摘要: 研究 O₃ 氧化对黄铜矿和辉钼矿浮选回收率的影响。单矿物浮选试验结果表明, 在 O₃ 浓度约为 90 g/m³、气体流量为 4 L/min 的条件下, 黄铜矿和辉钼矿氧化 2 min 后, 黄铜矿的浮选回收率降至 16%, 而辉钼矿的浮选回收率变化不大。人工混矿浮选试验结果表明, 在选择性浮选黄铜矿和辉钼矿中, O₃ 氧化预处理可以代替 Na₂S 试剂作为铜抑制剂。接触角测量结果表明, O₃ 氧化处理选择性地使黄铜矿表面具有亲水性。Zeta 电位和 X 射线光电子能谱分析结果表明, 氧化处理后黄铜矿表面产生不溶于水的亲水性氧化物和氢氧化物, 使得黄铜矿更加亲水; 此外, 辉钼矿的表面虽略有氧化, 但其表面仍保持疏水性。

关键词: 黄铜矿; 辉钼矿; O₃ 氧化; 选择性浮选; 亲水性

(Edited by Bing YANG)